CrystEngComm

Accepted Manuscript

ROYAL SOCIETY OF CHEMISTRY

www.rsc.org/crystengcomm

Cite this: DOI: 10.1039/c0xx00000x

www.rsc.org/xxxxxx

ARTICLE TYPE

Hydrogen Bond Synthon Competition in the Stabilization of Theophylline Cocrystals

Bipul Sarma,* and Basanta Saikia

Received (in XXX, XXX) Xth XXXXXXXXX 20XX, Accepted Xth XXXXXXXXX 20XX

DOI: 10.1039/b000000x

Theophylline medications are used as bronchodilators that relax the muscles in the breathing tubes. Issues relate to hydration behaviour, moisture stability of this drug, are well-familiar. Seven new cocrystals of theophylline with phenols, and isomeric hydroxybenzoic acids are synthesized. Solvent assisted mechanochemical synthesis is employed in order to synthesize cocrystal materials. Single crystal structures are obtained for all cocrystals and furthermore they are characterized thermally, spectroscopy and powder X-ray diffraction. The hydrogen bonding and crystal packing features are examined and found comparable to reported cocrystals/salts of theophylline or its molecular analogues, i.e. caffeine, and theobromine. The solubility of these cocrystals are determined using UV-Vis spectroscopy and correlated with the hydrogen bond synthon energies computed on Gaussian using DFT. Occurrence probability of hydrogen bond synthons are examined with Cambridge Structural Database (CSD). An important observation is that the phenol coformers facilitate water assimilation in the crystalline lattice since it offers a weaker O−H···$N_{imidazole}$ H bond synthon over a stronger COOH···$N_{imidazole}$ H-bond available in hydroxybenzoic acid coformers. Presence of –COOH group prevents water incorporation and provides added physical stability to the cocrystal yet at high humid condition. The results show the feasibility of cocrystal design of a drug to tune physical properties based on hydrogen bond synthons.

Introduction

Cocrystallizing an API with a pharmaceutically acceptable molecule has boosted the attractive route for developing pharmaceutical products.[1] Theophylline is an active pharmaceutical ingredient (API) analogous to caffeine and theobromine which belongs to the xanthine family.[2] It is used for the treatment of respiratory disease such as chronic obstructive pulmonary disease (COPD) and asthma under the brand name of Choledyl, Elixophyllin, Neulin, Theofyllin, Theochron SR etc. Theophylline behaves in a similar way to caffeine and theobromine towards atmospheric humidity.[3] The study on stability and interconversion of monohydrate and anhydrous theophylline is reported in the literature.[3] The presence of imidazole N as hydrogen bond acceptor interacts with atmospheric moisture and readily forms hydrate. Therefore the replacement of hydroxyl O−H···$N_{imidazole}$ weak hydrogen bond synthon by stronger COOH···$N_{imidazole}$ synthon, the instability of this molecule can be overcome. Synthesis of cocrystals[1i,4] specially of pharmaceutical relevance has proved to modulate solubility of parent drug by selecting suitable coformer based on H-bond principles,[5] and thereby solve drug delivery problems. Since last ten years or so, many researchers have been actively involved in investigating the property modulation of a drug by its cocrystal preparation, but the predictability of property of the drug-cocrystal based on hydrogen bonds and coformers is still indecisive. Jones *et. al*. have studied the hydration stability of caffeine and theophylline based on cocrystal preparation with different dicarboxylic acids.[3,4] They reported the theophylline and caffeine-oxalic acid cocrystals are the most stable among the studied cocrystals in all different relative humidity conditions. Rodriguez research group have extensively studied moisture uptake and deliquescence property by highly water soluble coformers for a series of API cocrystals with different relative humidity conditions.[3] The coformer like oxalic acid with high aqueous solubility exhibited the best cocrystal stability at high relative humidity. In contrast, the most soluble and hygroscopic coformers like D-malic acid is found unstable even at 75% RH leading to the hydrated drug.

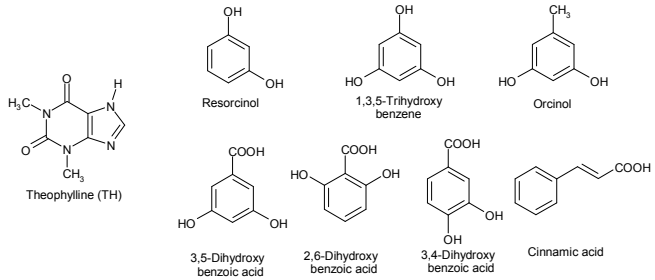

Scheme 1 Cocrystals of API theophylline prepared with phenols and isomeric dihydroxybenzoic acid coformers.

Recently, several novel examples of pharmaceutical cocrystals from the past decade are reviewed and analysed their enhanced solubility profile by Nangia *et. al*.[6] Apart from the advantages on

solubility or dissolution profile, physical stability of the drug always challenges the efficacy of the drug.

Carboxylic acid group (−COOH) that can act either as a hydrogen bond acceptor (=O, the carbonyl) or a hydrogen bond donor (−OH, the hydroxyl) and therefore a suitable molecular entity for cocrystal formation. The API theophylline behaves in identical manner, where the imidazole NH and =CH group act as hydrogen-bond donors and the two coordinate imidazole N and the two carbonyl oxygen atoms can act as hydrogen-bond acceptors.[7] Therefore cocrystal formation using O−H···O, N−H···O, O−H···N strong hydrogen bonds of theophylline, caffeine or theobromine with dicarboxyllic acids such as oxalic acid, maleic acid, glutaric acid;[8a] and dipicolinic acid, pyrazole dicarboxyllic acid, trimellitic acid[8b] have been the leading pick for researcher. Similar to –COOH, phenolic −OH group can also be used as s sensible co-crystal former. However phenols demand a compensation of hydrogen bond formation with theophylline which may be realizable by inclusion of water or solvent molecules into the crystalline lattice.

Table 1 Synthesis of seven new cocrystals of drug theophylline with phenols and isomeric dihydroxybenzoic acids with 1:1 ratio. Cocrystals **1**, **2**, **3**, **4** are hydrates.

Cocrystal	Components	Stoichiometry	Symbol
1	Theophylline+Resorcinol+H_2O	1:1:1	Theo•Res•H_2O
2	Theophylline+Phlouroglucinol+H_2O	1:1:1	Theo•Phu•H_2O
3	Theophylline+Orcinol+H_2O	1:1:2	Theo•Orc•$2H_2O$
4	Theophylline+2,6-Dihydroxybenzoic acid +H_2O	1:1:1	Theo•2,6-DHBA•H_2O
5	Theophylline+3,5-Dihydroxybenzoic acid	1:1	Theo•3,5-DHBA
6	Theophylline+3,4-Dihydroxybenzoic acid	1:1	Theo•3,4-DHBA
7	Theophylline+Cinnamic acid	1:1	Theo•CA

Several phenols such as resorcinol (Res), orcinol (Orc), phluroglucinol (Phu), and isomeric dihydroxybenzoic acids such as 2,6-dihydroxybenzoic acid (2,6-DHBA), 3,4-dihydroxybenzoic acids (3,4-DHBA), 3,5-dihydroxybenzoic acid (3,5-DHBA) are chosen as coformers in order to synthsize theophylline cocrystals (Scheme 1). Cinnamic acid (CA) is also used under the category of aromatic carboxylic acid with no –OH group. Seven new cocrystals are prepared and are characterized by spectroscopy, X-ray diffraction, their melting point recorded on DSC and TGA for water loss profile. Present investigation emphasizes the importance and understanding the factors that contribute to the modulation of physical stability of cocrystals of theophylline with isomeric dihydroxybenzoic acids compared to phenol coformers. Among isomeric dihydroxybenzoic acids; 3,4-DHBA and 3,5-DHBA are known to be tricky molecules as they readily produce inclusion complexes from solution crystallization.[9] This study of strategic coformer selection for cocrystal synthesis to modulate physical properties of theophylline drug is aimed with the following objectives, (i) liquid assisted grinding to promote new cocrystals synthesis, (ii) to achieve physical stability of cocrystals of theophylline even at high humid conditions that may improve efficacy and storage longevity of the parent drug, (iii) to determine solubility profile of the cocrystals and correlated to hydrogen bond synthon energies, and (iv) the emphasis on salt vs neutral cocrystals material synthesis based on ΔpK_a rules.[10] The role of coformers and thereby forming hydrogen bond synthons in determining the final cocrystal stability, hydration probability and modulating solubility profile is discussed.

Results and Discussion

Cocrystallisation of theophylline with 2,6-dihydroxybenzoic acid yielded ionic molecular complexes however other coformers gave neutral species. Several research groups have thoroughly investigated the occurrence of neutral or ionic hydrogen bond in acid-base complexes.[10b-c,11] The proton transfer behaviour in carboxylic acids and pyridine molecular complexes was emphasized on the difference in pK_a between the base and acid. The ΔpK_a < 0 and >4 for acids and bases resulted neutral hydrogen bond and proton transfer situations, respectively. When ΔpK_a lies between 0-4, the predictions about ionic and neutral states of resulting mixture is not confident. The fact that complex of saturated theophylline base (pK_a = 8.6) with 2,6-DHBA (pK_a = 1.26) is a salt, predicted by the larger ΔpK_a value. Four complexes were found hydrates i.e. **1**, **2**, **3**, **4**. Molecular packing and hydrogen bond synthon behaviour of these cocrystal materials in terms of donor-acceptor ratios are examined. The hydrogen bonding competition and other weak interactions define a specific motif for the crystallization of new solid form specially a desired polymorph and variable stoichiometry in multiple component systems have been emphasized elsewhere.[12] In all cocrystal materials we note that a 1:1 ratio of theophylline and coformer. Starting materials ratios 1:1.25; 1:1.5; 1:2; 2:1 of theophylline:coformer also resulted products of 1:1 stoichiometry and hydrates for **1-4**.

FT-IR spectroscopy

FT-IR spectroscopy is one of the popular analytical methods and used for studying hydrogen bond formation in the cocrystal materials. In the spectra of solid state samples, asymmetric and symmetric N−H stretching vibrations are observed in the range 3390−3323 cm^{-1} and 3279-3229 cm^{-1}, respectively, due to intermolecular hydrogen bonding. The O−H vibrations appear at 3600-3300 cm^{-1}. The C−N stretching vibrations of imidazole ring are observed within the range of 1350-1220 cm^{-1}, however C−N for pyrimidine ring absorbs at 1198, 1166, 1147, 1066 cm^{-1} etc. The N−H stretching vibrations are appeared at lower region due to extended hydrogen bonding in the cocrystal.[13] The C=O absorption are expected for theophylline at 1715 cm^{-1} and for the acid it is expected to be appear around 1730−1700 but we observed the absorption at lower frequency region due to participation of the C=O in hydrogen bonding. In the cocrystal **4,** the C=O absorption appeared at much lower region (1560 and 1404 cm^{-1}) can be assigned as the absorption due to the carboxylate ion, COO^- (Figure 1a and 1b).

Crystal Structure Analysis

Infantes *et. al*. have examined the factors determining hydrate formation in organic crystals. The donor/acceptor ratio or the molecular weight was not significantly affecting the hydrate formation. Perhaps increasing polar surface of the molecules was correlated with increasing hydrate formation. Presence of hydroxyl group in the molecule and specially their position in

hydroxybenzoic acids plays the key role in solvent inclusion. As reported in the literature cocrystal of theophylline with 2,4-DHBA, caffeine with 3,5-DHBA and theophylline with 2,6-DHBA (present study) are hydrate structure, whereas p-hydroxybenzoic acid, gentisic acid are two-component cocrystals. In the cocrystal structure of theophylline studied here show neutral conformation except the purine N is protonated in cocrystal **4**. The position of OH groups in isomeric dihydroxybenzoic acids plays an important role toward the inclusion of crystallizing media into the crystal lattice. Carboxylic acid homodimer formation in their solvated crystal structures were commonly observed except in dioxane solvate and guest free melt polymorph structures.[9] The two OH groups of 3,5-DHBA can adopt 4 possible conformations and the *anti-anti* conformation is present in cocrystal **5.** The uncommon *anti-anti* conformation of two hydroxyl groups of 3,5-DHBA is also observed in the guest free melt polymorph 3,5-DHBA (refcode WUYPOW) and cocrystal with caffeine (MOZCEK). The 3,4-DHBA forms carboxylic acid homodimer in cocrystal **6** but the acid dimer synthon is absent in cocrystals **4** and **5**. Crystal data parameters are given in table 2 and hydrogen bond matrices are listed in table 3 along with corresponding symmetry operations. The CIFs and ORTEP drawings (Figure S1a-g) are made available as Supp. Information.

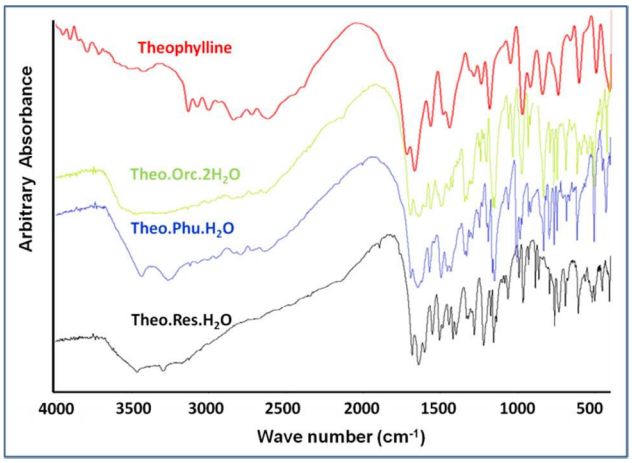

(a)

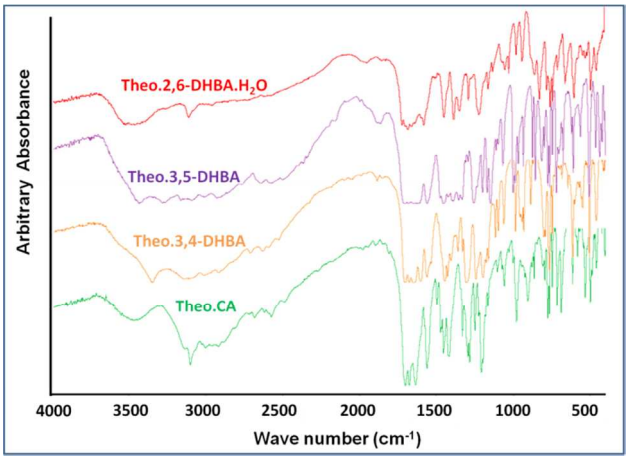

(b)

Figure 1 FT-IR spectra of theophylline base and cocrystals **1-3** (a) and **4-7** (b) in the full region of 400-4000 cm−1.

Theo•Res•H_2O [**1**]*:* Crystal structure shows one O−H group of resorcinol interacts with the *exo*-carbonyl of theophylline and imidazole N−H to the O of same OH group. The water molecule is incorporated to adjust H-bond donor-acceptor ratio and acts as a bridge which connects three theophylline molecules and one resorcinol molecule through O−H···O, O−H···N and N−H···O hydrogen bonds nearly in a tetrahedral arrangement (Figure 2a). The interaction between the resorcinol and theophylline resulted 3D packing of extended hydrogen bonding where the two components stacked with each other in an alternate fashion (Figure 2b).

Theo•Phu•H_2O [**2**]: Theophylline-phloroglucinol monohydrate single crystals can also be grown from EtOAc and EtOH solvents. Single crystal data were collected, solved and refined in $P2_1/c$ monoclinic space group. Absence of strong hydrogen bonding COOH group, the OH groups take part in hydrogen bonding with the *endo*-carbonyl group of theophylline molecule through O−H···O hydrogen bond. The other two O−H groups are connected through O−H···O hydrogen bond with water molecule and the adjacent phloroglucinol (Figure 3a). The imidazole N−H groups forms infinite tape through N−H···N hydrogen bond with the N1 atom of the adjacent theophylline molecule similar to the anhydrous forms (Figure 3b).

Theo•Orc•$2H_2O$ [**3**]: Crystal data were solved and refined in orthorhombic *Pbca* space group. There is no direct interaction between the theophylline and orcinol molecules in the crystal structure; rather they are connected via water molecules via a bifurcation of O−H···O hydrogen bond. Theophylline and orcinol molecules form infinite chains running parallel to each other (Figure 4a). Similar type of chain connecting the imidazole molecule of theophylline (synthon E, scheme2) can be seen in the anhydrous form of theophylline molecule. The 3D packing of the cocrystal is fulfilled by the water molecule connecting the layers formed via Orc and theophylline chains (Figure 4b).

Theo•2,6-DHBA•H_2O [**4**]: The 2,6-DHBA coformer resulted a salt structure of theophylline with 1:1 stiochiometry. It is a monohydrate, where the carboxylic proton is transferred to the imidazole N1 of theophylline molecule. The two hydroxyl groups of the 2,6-DHBA took part in intramolecular hydrogen bond with the carboxylate oxygen atoms. Bučar *et. al.* studied the involvement of intramolecular $O-H_{hydroxy}\cdots O_{carboxyl}$ hydrogen bond for *ortho*-hydroxy benzoic acid on cocrystallising with caffeine and inclusion of water molecule in the crystal structure. Due to the intramolecular H bond, the hydroxyl groups are unable to participate in intermolecular H bonding. The water molecule connects the theophylline dimer through O−H···O and N−H···O hydrogen bond (Figure 5a). The theophylline-2,6-DHBA forms a layer along (0 1 0) plane and the water molecule connects the 2D layers through O−H···O hydrogen bond as shown in the Figure 5b.

Table 2 Single crystal X-ray data parameter of cocrystals **1-7**

Crystal Data	[1] Theo• Res•H_2O	[2] Theo• Phu•H_2O	[3] Theo• Orc•$2H_2O$	[4] Theo•2,6-DHBA•H_2O	[5] Theo• 3,5-DHBA	[6] Theo• 3,4-DHBA	[7] Theo•CA
Formula unit	$C_7H_8N_4O_2$· $C_6H_6O_2$·H_2O	$C_7H_8N_4O_2$· $C_6H_6O_3$·H_2O	$C_7H_8N_4O_2$· $C_7H_8O_2$·$2H_2O$	$C_7H_8N_4O_2$· $C_7H_6O_3$·H_2O	$C_7H_8N_4O_2$· $C_7H_6O_4$	$C_7H_8N_4O_2$· $C_7H_6O_4$	$C_7H_8N_4O_2$· $C_9H_8O_2$
Formula wt.	308.30	324.30	340.34	352.31	334.29	334.29	328.33
Crystal system	Monoclinic	Monoclinic	Orthorhombic	Monoclinic	Triclinic	Triclinic	Monoclinic
T [K]	100	100	100	100	296	296	296
a [Å]	11.0728(4)	6.7236(3)	9.8095(15)	14.8098(5)	7.3213(2)	8.0940(5)	7.2792(7)
b [Å]	8.7248(4)	23.2123(9)	13.369(2)	6.6905(2)	8.0238(2)	8.5956(5)	8.7135(9)
c [Å]	14.6199(7)	9.2933(3)	23.858(4)	15.8509(6)	12.6902(2)	11.5891(5)	24.272(2)
α [°]	90	90	90	90	81.6460(10)	103.168(3)	90
β [°]	109.072(2)	98.822(2)	90	94.469(2)	85.6010(10)	105.023(5)	96.128(4)
γ [°]	90	90	90	90	82.1560(10)	105.320(4)	90
Volume [Å^3]	1334.87(10)	1433.25(10)	3128.9(8)	1565.81(9)	729.44(3)	712.05(7)	1530.7(3)
Space group, *Z*	*Cc*, 4	$P2_1/c$, 4	*Pbca*, 8	$P2_1/c$, 4	*P*-1, 2	*P*-1, 2	$P2_1/c$, 4
Dcalc [g cm^{-3}], μ/mm^{-1}	1.534, 0.120	1.503, 0.121	1.445, 0.114	1.494, 0.122	1.522, 0.122	1.559, 0.124	1.425, 0.105
Reflns. Collected, Unique, Observed	10271, 3196, 2751	20611, 7423, 4115	6568, 1602, 1358	36046, 6785, 3938	21150, 5826, 4276	19670, 5748, 3652	20479, 8056, 4961
*R*1 [I>2σ (I)], *wR*2, GOF	0.0291, 0.0849; 1.252	0.0617, 0.1474; 0.967	0.0381, 0.1076; 1.152	0.0575, 0.1670; 1.046	0.0486, 0.1381; 1.073	0.0753, 0.2037; 1.082	0.0777, 0.2043; 0.998

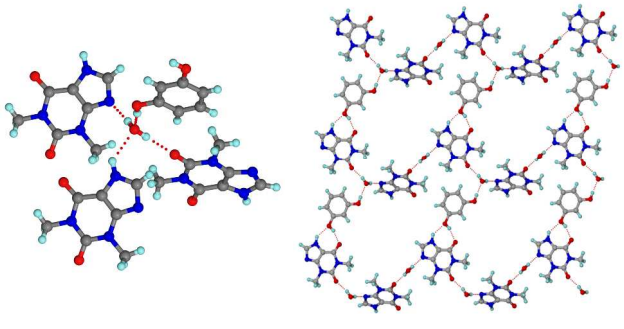

(a) (b)

Figure 2 (a) Water acts as connector via O−H···O, O−H···N and N−H···O hydrogen bonds in cocrystal **1**. (b) One of the –OH groups of resorcinol is hydrogen bonded to theophylline through O−H···O and N−H···O from imidazole NH which then extended through water linkage forming a 1D tape. The 1D tapes are connected by theophylline molecule through water linker form 2D net.

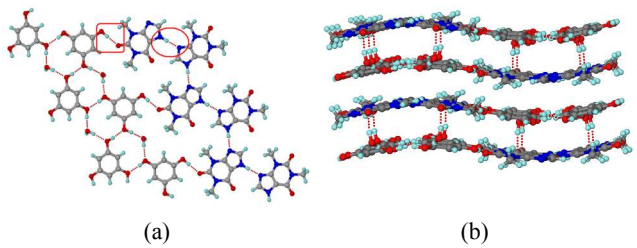

(a) (b)

Figure 3 (a) In cocrystal **2**, theophylline forms a catemeric N−H···N hydrogen bonds (synthon E listed in scheme 2) found uncommon in theophylline cocrystals. The catemeric N−H···N hydrogen bonds is assisted by weak C−H···O from imidazole =CH. (b) Water molecules connect the wavy 2D molecular sheets to complete 3D packing.

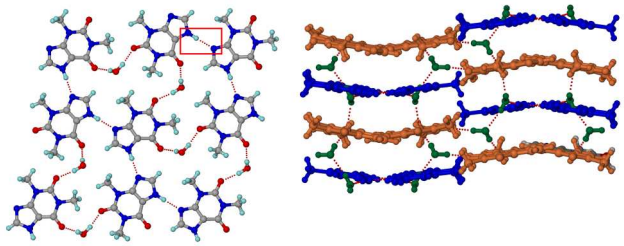

(a) (b)

Figure 4 (a) The theophylline molecules are arranged as catemeric N−H···N hydrogen bonds in cocrystal **3** similar in cocrystal **2**. (b) Water molecules act as hydrogen bonded connector of the 2D wavy molecular sheets formed by the API and coformer leading to 3D packing.

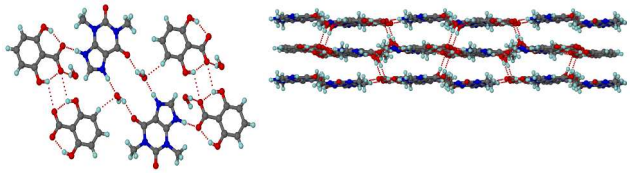

(a) (b)

Figure 5 (a) The –COOH proton from 2,6-dihydroxybenzoic acid is transferred and sits on the basic N centre of imidazole ring. The theophylline forms N−H···O dimer bridged by water molecule in **4** [Theo•2,6-DHBA•$2H_2O$]. Both –OH groups are engaged in intramolecular hydrogen bonding and water involves in assembling 2D layers of API and coformers into 3D structure (b).

Theo•3,5-DHBA [**5**]: Cocrystals of 1:1 stoichiometry of theophylline and 3,5-DHBA were crystallized out and single crystal data were determined. The –COOH group forms hydrogen bond (synthon A, Figure 6a) with the imidazole N atom similar to the reported cocrystals with the aliphatic dicarboxylic acids. Two of the theophylline molecule forms a dimer through N−H···O hydrogen bond between the *exo*-carbonyl O and imidazole N−H group similar to the monohydrate and the aliphatic dicarboxylic acid cocrystals. The second carbonyl group forms an O−H···O hydrogen bond with one of the hydroxyl groups of 3,5-DHBA. All the hydrogen bonding functional group are utilized in hydrogen bonding results a planar sheet parallel to (2 1 -1) plane (Figure 6b).

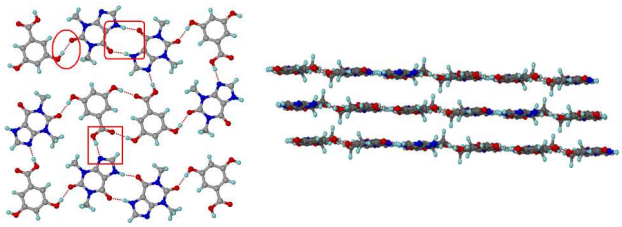

(a) (b)

Figure 6 (a) Involvement of all functional groups in hydrogen bonding permits no water inclusion. Theophylline forms N−H···O dimers and one of the –OH groups and C=O from 3,5-dihydrobenzoic acid form O−H···O dimers in cocrystal **5**. (b) 2D molecular layers are stacked via weak interactions like π···π and C−H···π that complete crystal structure.

Theo•3,4-DHBA [**6**]: Single crystal data of **6** were solved and refined in triclinic *P*-1 space group. The common synthons A, B or C are found absent in the crystal structure. Rather, carboxylic acid group of 3,4-DHBA forms a homodimer with an adjacent molecule. The two hydroxyl group interact with the theophylline molecule, one with the imidazole N atom forming an O−H···N hydrogen bond and the other with endo-carbonyl via discrete (D) O−H···O hydrogen bond synthon (Figure 7a). Theophylline dimer synthon D is present in this cocrystal as well as similar to that of cocrystal **5**. Hydrogen bonded theophylline-3,4-DHBA sheets stacked parallel to (-2 2 1) plane with the help of π-π interaction to fulfil the 3D packing (Figure 7b).

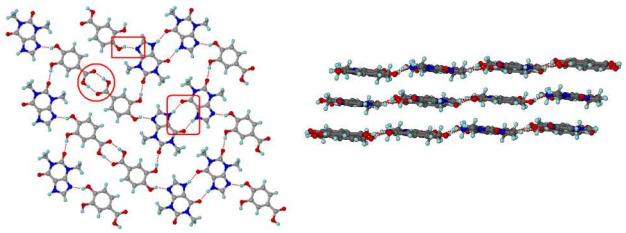

(a) (b)

Figure 7 (a) Carboxylic acid homo dimer is formed via O−H···O hydrogen bonds in addition to theophylline N−H···O dimers in cocrystal **6**. The two –OH groups were engaged in hydrogen bonding to connect two API via N−H···O dimer that forms a 2D molecular sheet further stacked through weak interaction into 3D packing (b).

Theo•CA [**7**]: Needle shaped crystals of theophylline and cinnamic acid cocrystals with 1:1 stoichiometry were obtained, solved and refined in monoclinic $P2_1/c$ space group. Unlike the theophylline-dicarboxylic acids cocrystals reported in the literature, cinnamic acid forms a carboxylic acid two-point synthon (synthon C) with *exo*-carbonyl O of pyrimidine ring, and the N−H hydrogen of the imidazole ring of theophylline (Figure 8a). Due to the presence of this strong N−H···O and O−H···O hydrogen bond synthon, hydrate formation is avoided. The discrete theophylline-CA dimers are connected via weak C−H···N interaction forming an infinite zigzag tape, stacked parallel to (1 0 -2) plane (Figure 8b) via π-π stacking.

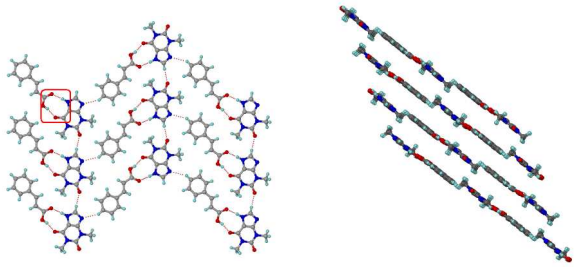

(a) (b)

Figure 8 (a) Carboxylic acid forms stronger 2 point acid···amide like synthon via O−H···O and N−H···O hydrogen bonds in cocrystal **7**. The API···coformer units are further assisted by weak C−H···N and C−H···O hydrogen bonds leading to 1D zig-zag chains. (b) The 2D molecular layers are stacked by weak interactions completes 3D arrangement of molecules.

Powder X-ray diffraction

Experimental PXRD patterns (Figure 9) of all seven theophylline co-crystals were compared with those simulated from the single-crystal structures. Reitvelt refinement[14] shows the same peak positions and patterns of intensities and exhibits good agreement with the simulated one. Overlay patterns are presented in supp. information (Figure S2a-g).

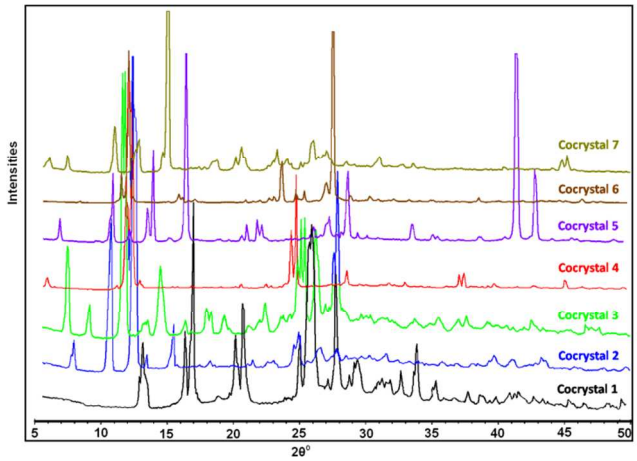

Figure 9 Powder X-ray diffraction patterns of cocrystals **1**-**7** show a new cocrystal phase entirely dissimilar from starting material PXRD patterns. The experimental PXRD patterns are overlaid with simulated from crystal structure individually and found good agreement after Reitvelt refinement presented in the Supp. Info (Figure S2a-g).

Thermal Analysis

Weight loss was observed by TGA and was an endotherm corresponding to water loss observed by DSC for all hydrate structures (Figure 10a). The onset of melting and peak observed by DSC for cocrystal materials were presented in table 4. For cocrystal 1 and 3 observed water loss and melting endotherms at relatively lower temperature, i.e. ~80 °C & ~50 °C and 101 °C & 109 °C respectively. An endotherm at 112 °C for cocrystal 2 indicates water loss however the cocrystal material melts at 153 °C. Recrystallization of this material followed by a second endotherm for cocrystal 2 at 169 °C was observed which may be due to a phase transformation into anhydrous or an unknown form. Detail structural characterization of this cocrystal material

after heating at 170 °C for 30 mins is pending.

Table 3 Hydrogen bond matrices for cocrystal **1-7** with symmetry codes.

Interaction	H···A/ Å	D···A/ Å	∠D–H···A/º	Symmetry code
1 [Theo•Res•H_2O]				
O3–H3···O1	1.75	2.680(2)	156	-1/2+x,-1/2+y,z
O4–H4···O5	1.72	2.697(2)	174	-
N4–H4A···O5	2.28	3.024(2)	130	x,1-y,-1/2+z
N4–H4A···O3	2.10	2.862(2)	131	1/2+x,1/2+y,z
O5–H5A···O2	1.83	2.777(2)	162	x,1+y,z
O5–H5B···N3	1.94	2.918(2)	175	1/2+x,1/2-y,1/2+z
C1–H1···O1	2.47	3.345(2)	137	-1/2+x,1/2-y,-1/2+z
C11–H11···O4	2.42	3.497(2)	173	-1/2+x,1/2-y,-1/2+z
2 [Theo•Phu•H_2O]				
N2–H2···N1	1.76	2.764(2)	180	x,1/2-y,1/2+z
O3–H3···O2	1.76	2.747(2)	178	1-x,-y,-z
O4–H4A···O6	1.66	2.640(2)	173	x,y,-1+z
O5–H5···O4	1.74	2.720(2)	172	x,1/2-y,1/2+z
O6–H6D···O5	1.85	2.809(2)	165	-
O6–H6E···O1	1.85	2.797(2)	160	-
C1–H1···O1	2.42	3.321(2)	139	x,1/2-y,-1/2+z
3 [Theo•Orc•$2H_2O$]				
N1–H2···N2	1.84	2.847(4)	172	-1/2+x,y,1/2-z
O3–H3···O6	1.65	2.628(4)	175	-1+x,y,z
O4–H4···O3	1.79	2.768(4)	173	1/2+x,y,1/2-z
O5–H5A···O2	1.81	2.781(4)	171	1/2+x,1/2-y,-z
O5–H5B···O1	1.84	2.813(3)	168	1+x,y,z
O6–H6D···O5	1.84	2.753(5)	152	-
O6–H6E···O1	2.29	3.008(4)	129	1/2-x,1/2+y,z
C1–H1···O1	2.44	3.218(4)	128	1/2+x,y,1/2-z
4 [Theo•2,6-DHBA•H_2O]				
N3–H3···O3	1.59	2.600(1)	177	x, 3/2-y,1/2+z
N4–H4···O7	1.67	2.678(2)	175	-x,1/2+y,1/2-z
O7–H7D···O1	1.92	2.848(2)	157	x,3/2-y,1/2+z
O7–H7E···O4	1.87	2.845(2)	173	x,1/2-y,1/2+z
C1–H1···O5	2.13	3.205(2)	175	-x,1/2+y,1/2-z
C6–H6A···O3	2.28	3.351(2)	169	x,3/2-y,1/2+z
C11–H11···O7	2.41	3.441(2)	158	-
C13–H13···O2	2.36	3.419(2)	165	1-x,-1/2+y,1/2-z
5 [Theo•3,5-DHBA]				
N2–H2···O1	1.74	2.734(1)	169	1-x,1-y,-z
O4–H4···N1	1.74	2.715(1)	174	-1+x,1+y,z
O5–H5···O2	1.75	2.734(1)	175	1-x,1-y,1-z
O6–H6···O3	1.82	2.799(1)	171	-x,1-y,-z
C1–H1···O6	2.37	3.442(2)	170	1-x,-y,-z
C10–H10···O2	2.44	3.221(1)	128	1-x,1-y,1-z
6 [Theo•3,4-DHBA]				
O3–H3···O4	1.66	2.639(2)	177	1-x,2-y,-z
N4–H4···O1	1.78	2.764(2)	165	1-x,1-y,-z
O5–H5···O2	1.72	2.701(2)	179	2-x,2-y,1-z
O6–H6···N3	1.87	2.746(2)	148	1-x,1-y,1-z
C7–H7A···O6	2.30	3.234(2)	143	1-x,1-y,1-z
C7–H7C···O5	2.38	3.421(2)	161	1+x,y,z
7 [Theo•CA]				
N2–H2···O4	1.76	2.761(2)	169	1-x,2-y,-z
O3–H3···O1	1.69	2.644(2)	164	1-x,2-y,-z
C1–H1···O2	2.11	3.186(2)	175	x,1+y,z
C7–H7B···N1	2.53	3.453(2)	143	2-x,-1/2+y,1/2-z

Water is lost in single endothermic step where the water molecule escapes at below 120 °C for all hydrated structures. Broad endotherm for cocrystal 3 corresponds for two water molecules lost at relatively low temperature. The total weight loss between 50–120 °C (Figure 10b) is consistent with monohydrate for cocrystals 1 (obs. 5.71%, calc. 5.83%), 2 (obs. 5.34%, calc. 5.53%), 4 (obs. 5.86%, calc. 5.11%) and dihydrate for cocrystal 3 (obs. 11.7%, calc. 10.5%) and confirmed by guest stoichiometry from the X-ray crystal structures.

Solubility Determination

Solubility of all cocrystal materials have been evaluated by using UV-Vis spectroscopy. Methods are described in the experimental section. Results show that the cocrystal **3** (34.50 mg/mL, 0.1014 mmol/mL) has over two times aqueous solubility than the drug theophylline. The cocrystal **1** (23.6 mg/mL, 0.076 mmol/mL) and **2** (27.20 mg/mL, 0.0839 mmol/mL) showed the similar trend. Aqueous solubility for cocrystal **4** is found to be 17.60 mg/mL (0.0526 mmol/mL) which is considerably higher than that of independent coformer 2,6-Dihydroxy benzoic acid i.e. 2.50 mg/mL (0.016 mmol/mL). The higher solubility can be attributed from the presence of water molecules in the lattice and the formation of weaker O−H···O intermolecular H−bonding. In addition cocrystal **4** is ionic in nature.

The dissociation of cocrystals in aqueous solution is commonly known to happen for many cocrystal systems that include a drug known to form hydrates. An important observation from single crystal structure of hydrated crystals is that, the water molecule plays a key role in bridging drug···drug and drug···coformer interaction. This in turn lowered the stability of these cocrystals and dissociate to its coformer and API. On the contrary, the non-hydrated cocrystals show considerably lower aqueous solubility because the presence of stronger intermolecular COOH···$N_{imidazole}$ H-bonding. Cocrystal **5** shows negligible aqueous solubility (0.14 mg/mL, 0.0004 mmol/mL). In cocrystal **6** the coformer 3,4-DHBA (12.4 mg/mL, 0.08 mmol/mL) is involved in carboxylic acid homodimer formation leaving only the –OH groups for weak intermolecular H−bonding with the API molecules. The cocrystal **7** falls into the same trend showing only 0.62 mg/mL aqueous solubility. The solubility of theophylline was measured and found 8.24 mg/mL (0.0457 mmol/mL) at 20 °C (Literature value 8.3 mg/mL, 0.0462 mmol/mL).

Physical Stability

To compare the stability of theophylline cocrystals **1**–**7** towards relative humidity conditions, an experiment of unit cell parameter checking by single crystal X-ray diffractometer was performed. Unit cell was determined at specific intervals over a time period of 3 months. Cocrystals **1**, **3**, **5**, **6** and **7** are considered for this assessment. A suitable single crystal from each system was subjected for the experiment. Same crystal was kept for one day at relative humidity (RH) 90% and determined the cell parameter again. The experiment was repeated for the crystal after 7 days and 90 days.

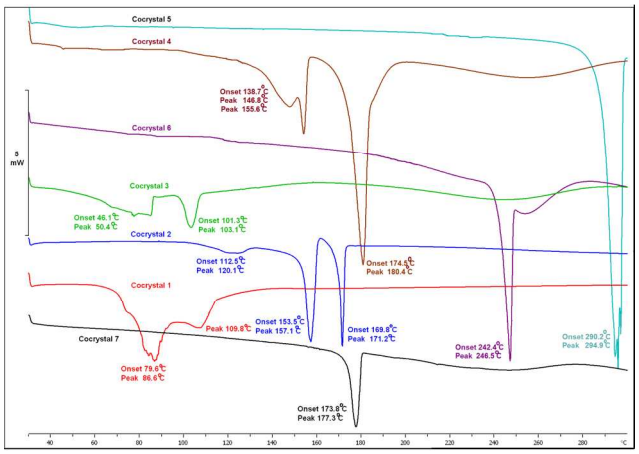

(a)

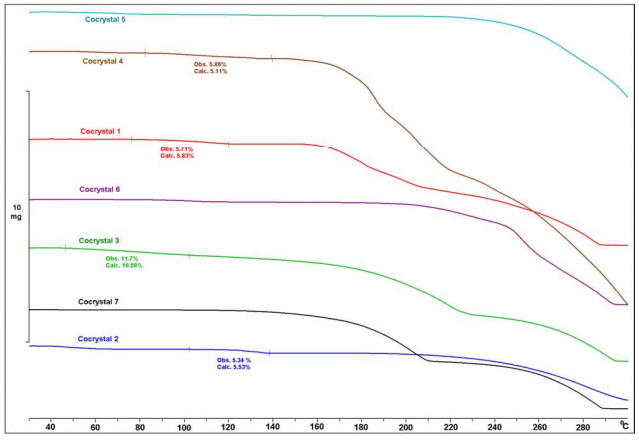

(b)

Figure 10 (a) Differential Scanning Calorimetry (DSC) of cocrystals **1**, **2**, **3** and **4** show corresponding endotherm for water loss. Water release occurs below 120 °C for the four hydrate structures. Melting temperature for all cocrystal materials were found different from starting materials. (b) Quantitative analysis of stoichiometric water in four hydrate structures (1, 2, 3, 4) by Thermo Gravimetric (TG) measurement was in accordance with 1:1 ratio determined by single crystal X-ray diffraction.

Table 4: DSC endotherm below 120 °C for hydrate cocrystals **1**, **2**, **3**, and **4** correspond to the water release. The endotherm representing melting onset of the cocrystal is utterly dissimilar from the API and coformer melting temperatures.

API	Coformer	Coformer melting (○C)	Cocrystals / salt	Water loss temperature (○C)		Cocrystal melting point (○C)	
				Onset	Peak	Onset	Peak
Theophylline [M.P. 271-272 °C]	Resorcinol	110-113	1	79.6	86.6	79.6	109.8
	Phloroglucinol	218-221	2	112.5	120.1	169.8	171.2
	Orcinol	106-112	3	46.1	50.5	101.3	103.1
	2,6-Dihydroxy benzoic acid	165-166	4	138.8	146.9	174.5	180.4
	3,5- Dihydroxy benzoic acid	235-238	5	-	-	290.2	294.9
	3,4 Dihydroxy benzoic acid	197-200	6	-	-	242.4	246.5
	Cinnamic acid	132-135	7	-	-	173.8	177.3

This test was performed in order to assess whether these cocrystals offer enhanced physical stability towards high moisture condition. It has already been investigated the high humid and/ or solution mediated transformation of anhydrous forms of theophylline to the hydrate formation specially monohydrate by the researcher using different methods.[3,4] Our observation says consistency of cell parameter over the time window of 3 months at 90% RH for the cocrystals **5**, **6** and **7** (Table 5 includes crystal unit cell parameter only for **5** & **6**). However the release/ reuptake of water molecules from the crystalline lattice of **1** and **3** destroy the crystalline property and thereafter the experiment was stopped for those samples. PXRD patterns of the cocrystal materials preserving at different RH and recorded time to time and then evaluation, thermo gravimetric analysis etc. would certainly predict the hydration profile. To shed light into water mediated cocrystal transformation into its coformers or drug as hydrate we present our qualitative result only for cocrystal **1** as the detail qualitative and quantitative study on hydration profile falls outside the scope of the present study. Bulk sample was kept at 90% RH and PXRD was evaluated time to time. The powder pattern recorded after 3 days depicts arrival of few new peaks at (2θ) 8.82, 11.64, 14.90, 27.51, 35.01 etc. All new peaks get better with intensity over time (at 7 days and so on) and they refer to the monohydrate of drug theophylline (Figure 12).

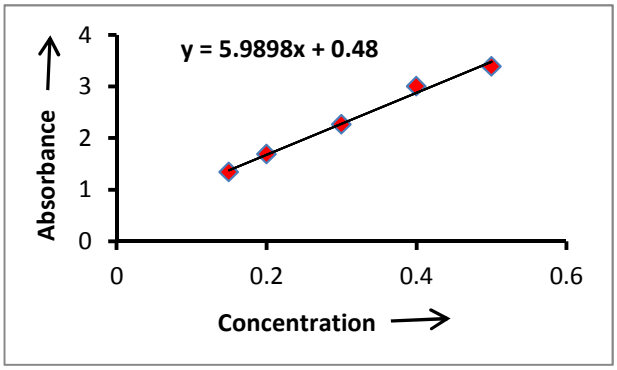

(a) Cocrystal **1**

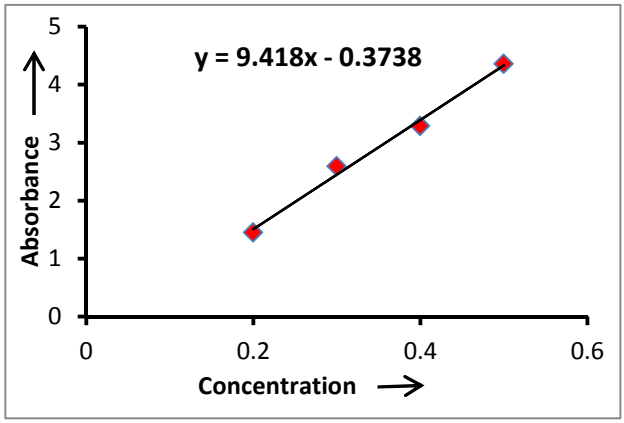

(b) Cocrystal **2**

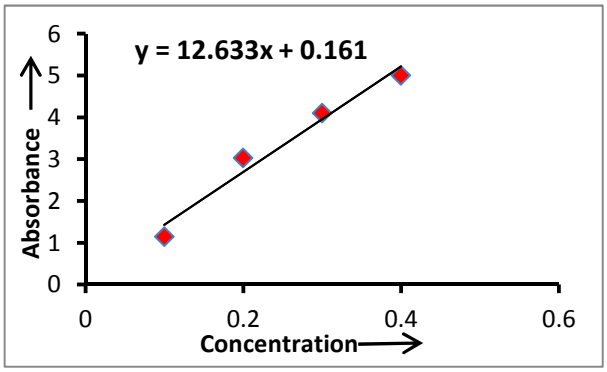

(c) Cocrystal **3**

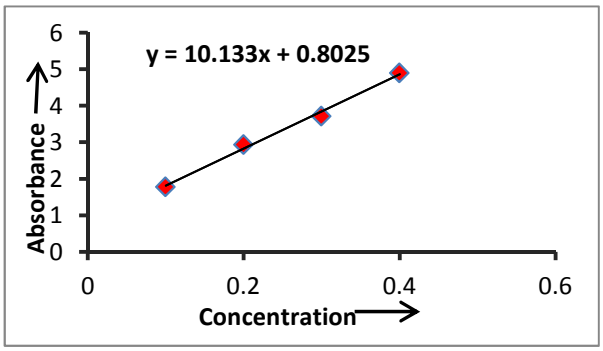

(d) Cocrystal **4**

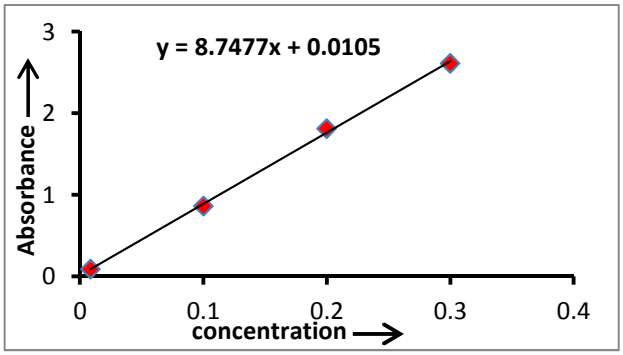

(e) Cocrystal **5**

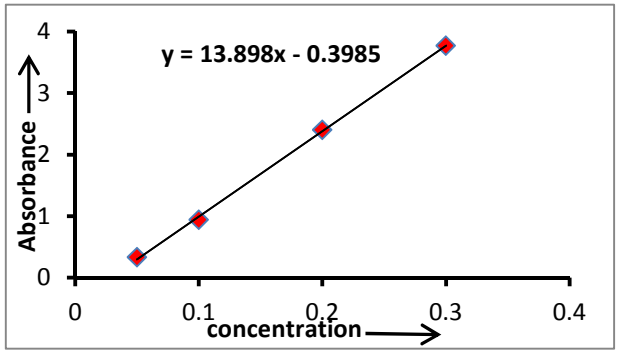

(f) Cocrystal **6**

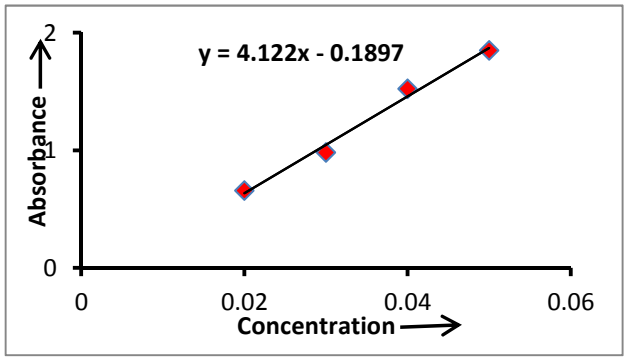

(g) Cocrystal **7**

Figure 11 (a) Solubility of cocrystals **1-7** are determined using UV-Vis spectra and pure API theophylline at 270 nm wavelength. Shown solubility calibration curves are evaluated with 0.1 mmol, 0.2 mmol, 0.3 mmol, 0.4 mmol standard solutions for each system. Detail method for determining calibration curve for the cocrystals is available in Supp. Info.

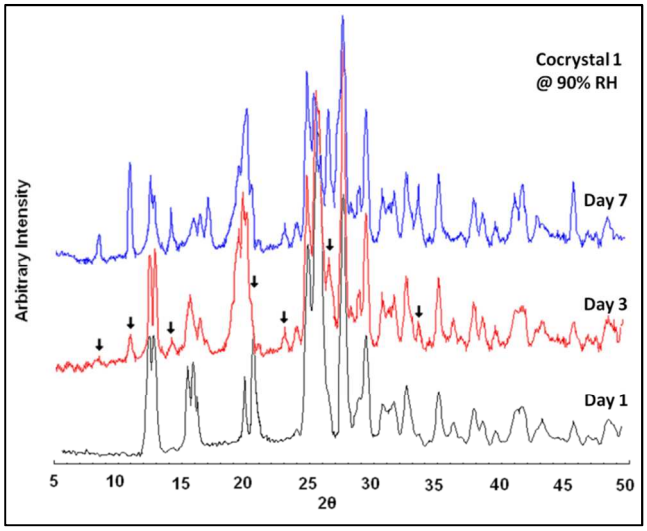

Figure 12 PXRD patterns of bulk sample of cocrystal **1** kept at relative humidity 90% show water mediated transformation into monohydrate of theophylline and the resorcinol. Arrival of new peaks after 3 days marked (pattern in red) is the indication of decomposition of cocrystal into its coformers and/or coformer hydrate.

Hydrogen bond synthon and CSD analysis

Hydrogen bonding and synthon competition among these cocrystals were accessed in terms of their synthon energy and analysed with CSD. Cambridge Structural Database (CSD)[15] search with "theophylline" fragment was carried out with 3D coordinates, restricted to organic molecules only. CSD version 5.34, May 2013 update was used in all searches, and crystal structures were visualized in Mercury 2.4. The lower R-factor structure was retained for duplicate refcodes. The search results total 51 hits. These structures were manually filtered to 30 crystal structures of which theophylline cocrystallized with aromatic carboxylic acids (14 hits), aliphatic carboxylic acids (11 hits) and with phenolic compounds (5 hits) and listed in table 7. None of the structure was found ionic except WUYRUD where the proton transfer has occurred from the $-SO_3H$ group.

Table 5 Physical stability of cocrystals was determined at 90% relative humidity by unit cell parameter determination of one crystal of each cocrystal material over a time span of 90 days. This experiment shows cocrystals **1**, **2**, **3** are not as stable as cocrystals with isomeric hydroxybenzoic acids at high humid condition. Cocrystals **1**, **3**, **5**, **6**, and **7** were subjected for this test.

Unit cell	Theo•3,5-DHBA [**5**]			Theo•CA [**6**]		
Time	RH 90% 1 day	RH 90% 7 days	RH 90% 90 days	RH 90% 1 day	RH 90% 7 days	RH 90% 90 days
Crystal system	Triclinic	Triclinic	Triclinic	Triclinic	Triclinic	Triclinic
T [K]	296	296	296	296	296	296
a [Å]	7.3335 (2)	7.3191 (4)	7.2998 (2)	8.0967 (4)	8.1252 (6)	7.9940 (5)
b [Å]	8.0398 (2)	8.0348 (3)	8.0468 (2)	8.6123 (4)	8.6098 (5)	8.5845 (5)
c [Å]	12.693 2 (2)	12.649 0 (4)	12.701 5 (2)	11.592 1 (4)	11.590 1 (5)	11.689 1 (5)
α [°]	81.694 5 (9)	82.001 2(9)	81.664 0 (7)	103.17 0 (3)	102.96 8 (3)	102.89 2 (3)
β [°]	85.610 1 (9)	85.532 1 (8)	85.591 0 (9)	104.98 6 (4)	104.96 3 (6)	105.29 3 (5)
γ [°]	82.169 9 (9)	82.200 3 (8)	82.164 8 (9)	105.09 8 (3)	105.76 2 (4)	105.44 0 (4)
Volume [Å^3]	729.44 (3)	738.34 (3)	735.67 (4)	721.82 (9)	717.76 (10)	719.23 (10)

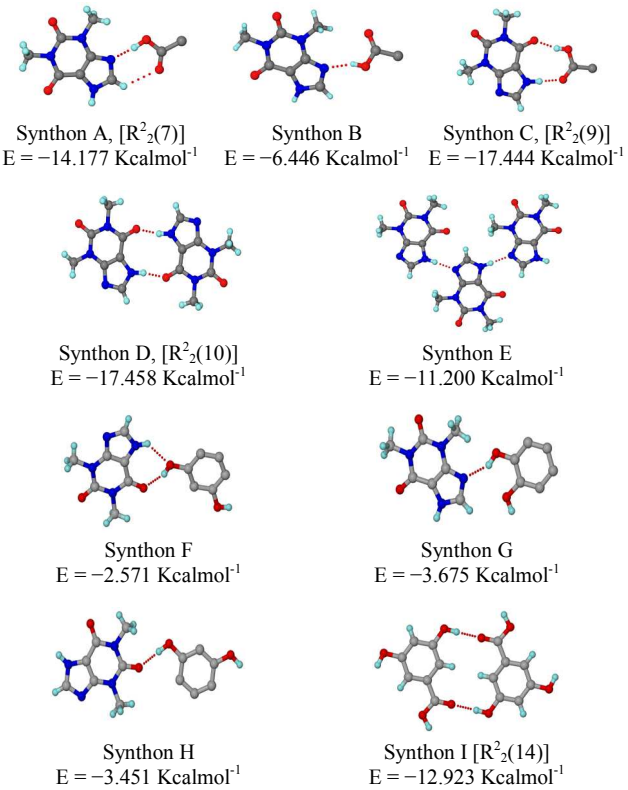

Scheme 2 Assorted hydrogen bonded synthons that are observed in the crystal structures of 1-7 between API theophylline and coformer functional groups such as –COOH and –OH. Two point theophylline N−H···O dimer (synthon D) and single point catemer synthon assisted by weak C−H···O (synthon E), two point (synthon A), single point (synthon B) −COOH···NHimidazole hydrogen bonds, and synthon C are assessed in terms of their stabilization energy which could translate into the physical stability of cocrystals. Synthon energies were calculated on DFT using Gaussian03 and B3LYP; 6311G*(d,p) as basis set. Probability occurrences of these synthons are compared with Cambridge Structural Database.

All the theophylline cocrystals with COOH groups were subdivided into three categories based on the supramolecular synthon present (Scheme 2). Out of the 25 cocrystals, 12 cocrystals contain imidazole-caboxylic acid two-point synthon A (48 %), 3 of them having imidazole-caboxylic acid one-point synthon B (12 %), whereas 8 cocrystals consists of carboxylic acid two-point synthon C, connecting exo-O of pyrimidine ring and imidazole N−H (32 %). Higher probability of synthon A is due to the formation of stronger hydrogen bond between imidazole and carboxylic acid group. Synthon C behaves like strong acid···amide like heterosynthon. Hydrogen bond synthon [presented in Scheme 2] energies were calculated with Gaussian03 (B3LYP/6-31G* (d,p)[16]. The COOH···N$_{imidazole}$ two point interaction in synthon A and C are found stronger than single point synthon B. High occurrence of synthon A and C in reported structures also supported the same. Setting up stronger interaction between API and coformers would certainly predict better physical stability of that cocrystal.

Another observation was that the aliphatic and aromatic acids with lower pK_a (< 4) prefer synthon A and B; whereas acids with moderate pK_a (≥ 4) and having hydrogen bond donor functionality at m/p position (aromatic acid) results synthon C. The competition between the carboxylic acid two point heterosynthon A and acid-triazole synthon B is compared with CSD database and correlated with pK_a of carboxylic acids. Stronger acids prefer synthon B and moderate to weak acids resulted formation of synthon A. The N−H···O dimer synthon D is formed as secondary synthon while synthon A is present. Absence of –COOH group and/or presence of –OH group normally lead to synthon D. Catemeric N−H···O formed by theophylline is not generally found except in LEDVOH and cocrystal **3** in this study. The large pK_a difference of 2,6-DHBA (pK_a = 1.26) and theophylline (pK_a = 8.6) led to proton transfer. Though extensive hydrogen bonding exists within the structures, it is observed that the phenols are not suitable coformers to prevent hydration of theophylline cocrystals. Indeed the weaker –OH···N$_{imidazole}$, –OH···O promote incorporation of crystalline water resulted higher aqueous solubility and very low moisture stability. However hydroxybenzoic acids are found better choice to provide superfluous stability to the API. The stronger –COOH···N$_{imidazole}$ heterosynthon presence is considered responsible for the enhancement of properties.

Table 6 Hydrogen bond synthon of theophylline cocrystals compared with CSD. Coformers selected as aromatic and aliphatic carboxylic acids and phenols. Synthon A and C refer to scheme 2 are found quite common in crystal structures. Presence of –OH groups facilitate the formation of N−H···O homo dimmers of the API theophylline.

Aromatic –COOH group		Aliphatic –COOH group		–OH group	
Refcode	Synthon	Refcode	Synthon	Refcode	Synthon
LEDVOH	E	CIZTAH	A	GAFTUE	D, G, H
VAXSAQ	C	CODCOO	A	KIGLUI	D
CSATEO	A, D	KIGKAN	-	KIGLUI01	D
DEYREF	C	KIGLAO	C	HEBFEB	D, H
DUCROJ	A, D	NEXWOD	B	HEBFIF	D, H
IJIBEJ	C, H	NEYCIE	B, D		
IJIBEJ01	C, G	WUYROX	-		
KIGLES	A, D	XEJWUF	B, D		
KIGLIW	A, D	XEJXAM	A, D		
KIGLOC	C, G	XEJXEQ	A, D		
LUKXUL	A, C	XEJXIU	A, D		
UNITER	A, C				
UNITIV	A				
WUYRUD	-				

Conclusion

Synthesis of pharmaceutical cocrystals based on hydrogen bond principles during the last decade to modulate physical properties of drug specially the solubility and dissolution profile became the high practice among pharmaceutical researcher. Perhaps poor moisture stability of many drugs create frequent nuisance. This study deals with strategic physical property modulation of cocrystals of bronchodilator drug theophylline synthesized mechanochemically. Two sets of coformers belonging to phenol and isomeric dihydroxybenzoic acid classes were chosen, known that they form weaker and stronger H bond with the API respectively and reasoned by CSD analysis and synthon energy calculation using DFT. An important observation is that the presence of weaker H bond and unmatched donor-acceptor ratios facilitate water assimilation into the crystal lattice. This in fact reflected in low moisture stability and high aqueous solubility of cocrystals with phenols determined experimentally. Similarly, a sharp decrease in solubility for cocrystals with isomeric hydroxybenzoic acids is observed and correlated with the presence of stronger hydrogen bonds. Physical stability towards high relative humidity is checked by single crystal unit cell parameter determination over a time period of 90 days and found extremely stable with isomeric hydroxybenzoic acids. The role of functional group in cocrystal leading to different hydrogen bond synthon formation and their correlation with physical properties is awfully important in drug development.

Experimental Section

Preparation of cocrystals: Theophylline and coformers listed in Scheme 1 were purchased from Sigma Aldrich and used as received without further purification. Equivalent amount of theophylline and each coformer were individually taken in a mortar and ground with pestle for around ~45 minutes with drop wise addition of CH_3CN. The mixture was transferred into a vial and dissolved in a 1:4 mixture of CH_3OH and $CHCl_3$ with ~50 °C warm condition. Solution was then allowed for cocrystallization at room temperature with slow evaporation. Suitable crystals for single crystal data collection were crystallized out in 2-3 days. Rod and needle shaped crystals were grown for the cocrystal of Theophylline with Orc and CA otherwise block transparent crystals were common for the rest. Solvents from Merck and water filtered through a double deionized purification system (Milli Q Plus Water System from Millipore, USA) were used for necessary experiments. Crystals were then subjected for spectroscopic, thermal and X-ray diffraction analysis. The drug:coformer ratio in cocrystals **1** to **7** are found in 1:1. With phenolic coformers by slow evaporation of solution are found inefficient cocrystal synthesis and therefore rigorous grinding is necessary to give the product cocrystals. Being deficient in hydrogen bond acceptor property by phenols could result inefficient intermolecular interactions between molecules. Therefore hydrogen bond donor-acceptor ratio is adjusted for these cocrystals by inclusion of water molecules into crystalline lattice. Mechanochemical synthesis[17a-c] or cogrinding are known to be the classical methods to prepare molecular complexes that promotes the formation of microcrystalline seeds of the cocrystals in the solution to grow single crystals for X-ray diffraction. Indeed, we realized such liquid-assisted grinding as a powerful methodology to construct cocrystals in a rapid and quantitative manner.

Vibrational Spectroscopy: A Nicolet 6700 FT-IR spectrometer with a NXR FT-Raman Module was used to record IR spectra. IR spectra were recorded on samples dispersed in a KBr pellet. All major stretching vibrations for cocrystals **1**-**7** are; Theo•Res•H_2O (**1**): 3465 (O−H), 3292 (NH), 1683 (C=O, C=N), 1521 (C=C, C=O), 1329 (C−N), 1282 (C−N, w), 1220 (C−N), 863 (N−C−H) cm^{-1}; Theo•Phu•H_2O (**2**): 3431(OH), 3261 (N−H), 1692 (C=O, C=N), 1571 (C=O), 1329 (C−N), 1294 (C−O), 832 (N−C−H) cm^{-1}; Theo•Orc•$2H_2O$ (**3**): 3472 (OH), 1693 (C=O, C=N), 1341 (C−N), 863 (N−C−H) cm^{-1}; Theo•2,6-DHBA•H_2O (**4**): 3345 (O−H), 3137 (N−H), 1698 (C=O, C=N), 1560 (COO^-), 1404 (COO^-), 1328 (C−N), 1302 (C−O), 1220 (C−N), 884 (N−C−H) cm^{-1}; Theo•3,5-DHBA (**5**): 3431 (O−H), 3277 (N−H), 1685 (C=O, C=N), 1559 (C=O), 1353 (C−N), 1330 (C−O), 1256 (C−N), 855 (N−C−H) cm^{-1}; Theo•3,4-DHBA (**6**): 3460 (O−H), 3108 (N−H), 1684 (C=O, C=N), 1348 (C−N), 1292 (C−O), 1220 (C−N), 859 (N−C−H) cm^{-1}; Theo•CA (**7**): 3460 (O−H), 3098 (N−H), 1700 (C=O, C=N), 1560 (C=O), 1328 (C−N), 1283 (C−O), 1220 (C−N), 863 (N−C−H) cm^{-1}.

Powder X-ray diffraction: Powder XRD of all samples was recorded on a PANlytical 1830 (Philips Analytical) diffractometer using Cu-Kα X-radiation (λ = 1.54056 Å) at 35 kV and 25 mA. Diffraction patterns were collected over a 2θ range of 5-50° at a scan rate of 5° min^{-1}. The Powder Cell 2.3 program was used for Rietveld refinement.

Thermal Analysis: DSC and TGA were performed on a Mettler Toledo DSC 822e module and a Mettler Toledo TGA/SDTA 851e module, respectively. Samples were placed in open alumina pans for TGA and in crimped but vented aluminum sample pans for DSC. A typical sample size is 4-6 mg for DSC and 9-12 mg for TGA. The temperature range was 30-300 °C at 2 $Kmin^{-1}$ for DSC and 10 $Kmin^{-1}$ for TGA. Samples were purged with a stream of dry N_2 flowing at 150 mL min^{-1} for DSC and 50 mL min^{-1} for TGA.

X-ray Crystallography: X-ray reflections were collected on a Bruker SMART CCD diffractometer using Mo Kα (λ =0.71073 Å) radiation. Data reduction was performed using Bruker SAINT software.[18a] Intensities for absorption were corrected using SADABS. Structures were solved and refined using SHELXL-2008[18b] with anisotropic displacement parameters for non-H

atoms. Hydrogen atoms on O and N were experimentally located in all crystal structures. All C-H atoms were fixed geometrically using the HFIX command in SHELX-TL. X-Seed[18c] was used to prepare figures and packing diagrams. A check of the final CIF file using PLATON[18d,e] did not show any missed symmetry. The crystallographic parameters for all structures are summarized in table 2. The hydrogen bond distances in the X-ray crystal structures (table 3) are neutron-normalized by fixing the D-H distance to its accurate neutron value (O-H 0.983 Å, N-H 1.009 Å, C-H 1.083 Å). Crystallographic cif files (CCDC Nos. 958476-958482) are available at www.ccdc.cam.ac.uk/

DFT Computations: Hydrogen bond synthon energies were calculated with Gaussian03 (B3LYP/6-31G* (d,p).[16] Observed conformations and orientations of molecules in the crystal structure were considered for the energy calculation without further optimization to the gas phase minimized conformers.

Solubility Determination: A series of standard solution (i.e. concentration 0.1 mmol, 0.2 mmol, 0.3 mmol, 0.4 mmol etc.) of cocrystals were prepared in water to construct absorbance versus concentration calibration curve for each cocrystal material (Figure 11). The experiment was run for triplicate for consistency. An excess amount of each cocrystal was added individually to 20 mL of water in a jacketed, circulating flask maintained at 25 °C. Cocrystals (**1, 2** & **3**) with phenol coformers and **4, 5, & 6** with isomerichydroxybenzoic acid coformers and **7** with cinnamic acid were considered for aqueous solubility study[19] using UV-Vis spectrometry. The suspension was kept for overnight stirring. After filtering through a syringe filter of 0.45 µm size, the absorbance was determined by measuring the ultraviolet (UV) absorption at 270 nm.

All experiments were performed in HALO DB-30 UV−Visible double beam spectrophotometer. The experiment for unknown concentration solution was also repeated for three times. The concentration of the unknown solution (C_u) of the cocrystal was evaluated from the slope and intercept of the calibration curve by using the formula C_U = (A_U-INTERCEPT)/SLOPE, where A_U is the absorbance of the unknown solution (Figure 11a). To compare solubility data extracted from UV-Vis calibration curves we again performed gravimetric measurement for solubility determination. A fixed volume (2 mL) of individual sample was taken at regular interval, and the concentration was determined gravimetrically with a good agreement measured by UV-Vis.

Notes and references

*Department of Chemical Sciences, Tezpur University, Tezpur-784028, India. Fax: +91-3712-267005/6; Tel: +91 94357 58147; *E-mail: sarmabipul@gmail.com, or, bcsarma@tezu.ernet.in*

† Electronic Supplementary Information (ESI) available: [ORTEP drawings, overlaid PXRD patterns with simulated from single crystal structure, methods for solubility determination and crystallographic files (cif) of cocrystals **1-7** are available free of charge via the Internet at http://rsc.org]. See DOI: 10.1039/b000000x/

Acknowledgment: We thank the UGC for research funding, Department of Chemical Sciences, and Sophisticated Analytical Instruments Centre (SAIC), Tezpur University for providing instrumentation and infrastructure facilities. Prof. Ashwini Nangia, Ranjit Thakuria and Progyashree Goswami are thanked for technical discussion.

Reference:

1 (a) G. R. Desiraju, *Crystal Engineering: The Design of Organic Solids*; Elsevier: Amsterdam, 1989; (b) FDA Guidance (draft), December 2011: *Regulatory Classification of Pharmaceutical Co-Crystals*; (c) J. I. Wells, *Pharmaceutical Preformulation.* 2nd ed.; Ellis Horwood: Chichester, 1993; (d) W. Jones in *Organic Molecular Solids*, ed. W. Jones, CRC Press, New York, 1997, 149–199; (e) Ö. Almarsson, M. J. Zaworotko, *Chem. Commun.,* 2004, 1889−1896; (f) P. Vishweshwar, J. A. McMahon, J. A. Bis, M. J. Zaworotko *J. Pharm. Sci.,* 2006, **95**, 499−516; (g) N. Blagden, M. de Matas, P. T. Gavan, P. York, *Adv. Drug Delivery Rev.,* 2007, **59**, 617−630; (h) A. V. Trask, *Mol. Pharmaceutics,* 2007**, 4**, 301−309; (i) N. Schultheiss, A. Newman, *Cryst. Growth Des.,* 2009, **9**, 2950−2967; (j) D. J. Good, N. Rodriguez-Hornedo, *Cryst. Growth Des*., 2009, **9**, 2252−2264; (k) J. Chen, B. Sarma, J. M. B. Evans, A. S. Myerson, *Cryst. Growth Des*., 2011, **11**, 887–895; (l) B. Sarma, J. Chen, H. Y. His, A. S. Myerson, *Kor. J. Chem. Eng.,* 2011, **28**, 315−322; (m) M. J. Zaworotko *et.al. Cryst. Growth Des.,* 2012, **12**, 2147−2152.

2. (a) A. J. Wilson, P. G. Gibson, J. Coughlan, *The Cochrane database of systematic reviews* CD001281, 2000; (b) Y. Yano, M. Yoshida, S. Hoshino, K. Inoue, H. Kida, M. Yanagita, T. Takimoto, H. Hirata, T. Kijima, *Biochem. Biophy. Res. Commun*., 2006, **341**, 684–690.

3. (a) A. V. Trask, W. D. S. Motherwell, W. Jones, *Cryst. Growth Des.*, 2005, **5**, 1013−1021; (b) A. Jayasankar, N. Rodríguez-Hornedo, *Mol. Pharmaceutics*, 2007, **4**, 360−372; (c) A. Jayasankar, L. Roy, N. Rodríguez-Hornedo, *J. Pharm. Sci.*, 2010, **99**, 3977−3985; (d) H. D. Clarke, K. K. Arora, H. Bass, P. Kavuru, T. T. Ong, T. Pujari, L. Wojtas, M. J. Zaworotko, *Cryst. Growth Des.*, 2010, **10**, 2152−2167; (e) A. M. C. Cassidy, C. E. Gardner, W. Jones, W. *Int. J. Pharm.* 2009, **379**, 59–66; (g) A. V. Trask, *Mol. Pharmaceutics*, 2007, **4**, 301−309.

4. (a) G. R. Desiraju, *CrystEngComm,* 2003, **5**, 466; (b) A. D. Bond, *CrystEngComm,* 2007, **9**, 833; (c) M. J. Zaworottko *et. al. Cryst. Growth Des.,* 2012, **12**, 4290–4291.

5. (a) M. C. Etter, *Acc. Chem. Res.,* 1990, **23**, 122−126; (b) M. C. Etter, *J. Phys. Chem.,* 1991, **95**, 4601−4610; (c) G. R. Desiraju, *Angew. Chem. Int. Ed.,* 1995, **34**, 2311–2327; (d) G. R. Desiraju, *J. Am. Chem. Soc.,* 2013, **135**, 9952−9967.

6. N. J. Babu, A. Nangia, *Cryst. Growth Des*., 2011, **11**, 2662–2679 and references therein.

7. J. R. Cox, *Angew. Chem. Int. Ed.,* 2007, **46**, 1988−1991.

8. (a) A. V. Trask, W. D. Motherwell, W. Jones, *Int. J. Pharm.,* 2006, **320**, 114−123; (b) B. Das, J. B. Baruah, *Cryst. Growth Des.,* 2011, **11**, 278−286.

9. B. Sarma, P. Sanphui, A. Nangia, *Cryst. Growth Des.,* 2010, **10**, 2010−2389.

10. (a) K. –S. Huang, D. Britton, M. C. Etter, S. R. Byrn, *J. Mater. Chem.,* 1997, **7**, 713−720; (b) B. R. Bhogala, A. Nangia, *Cryst. Growth Des.,* 2003, **3**, 547-554; (c) B. Sarma, N. K. Nath, B. R. Bhogala, A. Nangia, *Cryst. Growth Des*., 2009, **9**, 1546–1557.

11. S. L. Childs, G. P. Stahly, A. Park, *Mol. Pharmaceutics*, 2007, **4**, 323–338.

12. B. Sarma, L. S. Reddy, A. Nangia, *Cryst. Growth Des*., 2008, **8**, 4546−4552.

13. (a) S. Gunasekaran, G. Sankari, S. Pommusamy, *Spectochemical Acta, Part A*, 2005, **61**, 117−127.

14. H. M. Rietveld, *J. Appl. Crystallogr.,* 1969, **2,** 65–71.

15. Cambridge Structural Database, CSD, version 5.34, ConQuest 1.15, November 2012 release, May 2013 update.

16. Gaussian 03 and Gauss View is the latest in the series of electronic structure and energy computation programs, www.gaussian.com.

17. (a) S. Karki, T. Friščić, W. Jones, W. D. S. Motherwell, *Mol. Pharmaceutics*, 2007, **4**, 347−354; (b) S. L. James, *Chem. Soc. Rev*., 2012, **41**, 413−447; (c) A. Delori, T. Friščić, W. Jones, *Crys.Eng.Comm.*, 2012, **14**, 2350−2362.

18. (a) SAINT Plus (Bruker AXS Inc.: Madison, WI, 2008; (b) BRUKER AXS (v 6.14); Bruker AXS Inc.: Madison, WI, 2008; (c) L. J. Barbour, *X-Seed, Graphical Interface* to SHELX-97 and POVRay;

University of Missouri-Columbia: Columbia, MO, 1999; (d) PLATON, A Multipurpose Crystallographic Tool; A. L. Spek, Utrecht University: Utrecht, Netherland, 2002; (e) A. L. Spek, *J. Appl. Crystallogr.,* 2003, **36**, 7−13.

19. (a) R. D. B. Walsh, M. W. Bradner, S. Fleischman, L. A. Morales, B. Moulton, N. Rodríguez-Hornedo, M. J. Zaworotko, *Chem. Commun.,* 2003, 186−187; (b) J. F. Remenar, S. L. Morissette, M. L. Peterson, B. Moulton, J. M. MacPhee, H. R. Guzman, Ö. Almarsson, *J. Am. Chem. Soc.,* 2003, **125**, 8456; (c) L. Childs, L. J. Chyall, J. T. Dunlap, V. N. Smolenskaya, B. C. Stahly, P. G. Stahly, *J. Am. Chem. Soc.,* 2004, **126**, 13335; (d) P. M. Bhatt, N. V. Ravindra, R. Banerjee, G. R. Desiraju, *Chem. Commun.,* 2005, 1073−1075; (e) A. Nangia, N. Rodríguez-Hornedo, *Cryst. Growth Des.,* 2009, **9**, 3339–3341.

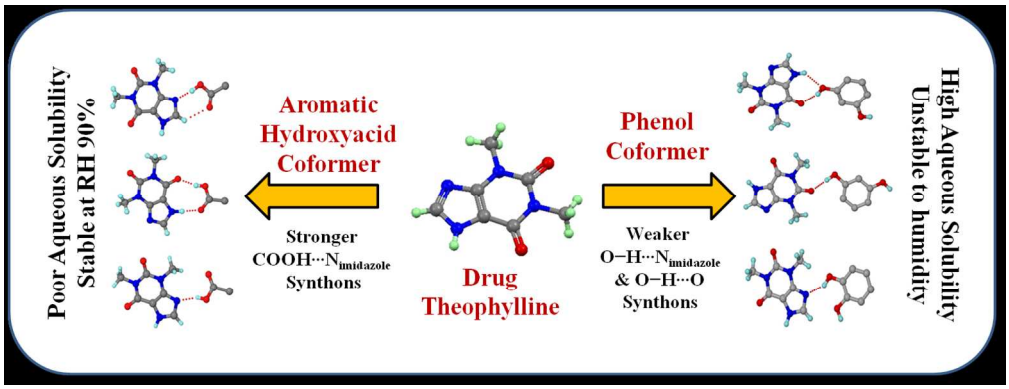

In the preparation of theophylline cocrystal, phenol coformers facilitate water assimilation in the crystalline lattice since a weaker O–H•••N(imidazole) synthon over a stronger COOH•••N(imidazole) H-bond. Presence of –COOH group prevents water incorporation and provides added physical stability to the cocrystal yet at high humid condition. This study of strategic coformer selection demands the feasibility of cocrystal design of an API to tune physical properties based on hydrogen bond synthons.
258x98mm (150 x 150 DPI)